# Metalloid cluster compounds of germanium: novel structural motives on the way to elemental germanium!

**Andreas Schnepf***

*Received (in Montpellier, France) 7th April 2010, Accepted 24th May 2010*
**DOI: 10.1039/c0nj00263a**

Metalloid cluster compounds of germanium of the general formulae $Ge_nR_m$ with $n > m$ (R = ligand), where naked as well as ligand bound germanium atoms are present, represent a novel class of cluster compounds in group 14 chemistry, being ideal model compounds to get an insight into the area between the molecular and solid state. This borderland is of particular interest, especially for metals or semimetals, as drastic changes of physical properties take place during reduction from salt-like oxidized species (*e.g.* oxides, halides: non-conducting) to the bulk elemental phase (metal: conducting; semimetal: semiconducting). Therefore, interesting properties are expected for these intermediate compounds which might complement results from nanotechnology. During the last years a couple of different syntheses have been introduced, leading to metalloid clusters of germanium which exhibit new structures and bonding. In this review an account is given on the first steps in this novel field of group 14 chemistry. Special attention is focused on structural features and bonding properties.

## 1. Introduction

Due to recent progress in nanotechnology and as a result of the miniaturization in industry the area between the molecular and solid state gets more and more into the focus of basic research.[1] Especially in the case of metals or semimetals drastic changes are expected during reduction from salt-like oxidized species (*e.g.* oxides, halides: non-conducting; *e.g.* $AlCl_3$, $AuCl_3$, $SiCl_4$, $GeO_2$ *etc.*) *via* metalloid clusters of the general formulae $M_nR_m$ ($n > m$; M = metals like Al, Au *etc.*; R = ligands like $S–C_6H_4–COOH$, $N(SiMe_3)_2$ *etc.*) to the bulk elemental phase (metal: conducting; semimetal: semiconducting; *e.g.* elemental Al, Au or Si).[2] This behaviour is quite different from that of "salt-like" cluster compounds *e.g.* a heterocubane $Na_4Cl_4·4D$ (D = $O{=}P(NMe_2)_3$, $Et_2O$) structure[3] can be seen as a fragment of the rock salt structure. Hence, in the case of "salt-like" clusters, already small clusters with only a small number of metal atoms (ions) exhibit a structure like that of the bulk material; *e.g.* $MO_6$ octahedra in poly-oxo-metallates (M = V, Ni, Mo, W)[4] or hexagonal closed packed (A–B–A) assemblies of selenium ions with copper ions in tetrahedral sites in $(Cu_2Se)_n$ clusters.[5]

This difference between "salt-like" and metalloid clusters is the result of the fact that in the case of metalloid clusters the oxidation state of the metal atoms inside the cluster changes, reaching more and more the value zero when the cluster gets larger and larger. Hence, metalloid cluster compounds can be seen as model compounds for the area between molecules and the solid state of metals and semi-metals. Despite this, in the case of salt-like clusters the oxidation state of the metal atoms (ions) is always the same. The highly mixed valence situation in the case of metalloid clusters leads to a complex bonding situation, which can directly be seen in the formation of novel structural motives.[6] Consequently, the arrangement of the metal atoms in a metalloid cluster cannot be described as a fragment of the solid state structure of the element.

This circumstance became more and more obvious in recent years as even the molecular structure of the largest metalloid cluster compounds structurally characterized *via* X-ray crystal structure analysis shows substantial differences of the arrangement of the atoms with respect to those found in the bulk material; *e.g.* the arrangement of the 84 gallium atoms in the metalloid cluster compound $Ga_{84}[N(SiMe_3)_2]_{20}^{x-}$ ($x$ = 3, 4)[7] only shows in the centre with a $Ga_2$ dumbbell a minor resemblance to the

---

*Karlsruhe Institute of Technology (KIT), Institute of Inorganic Chemistry, Engesserstraße 15, Geb. 30.45, D-76131 Karlsruhe, Germany. E-mail: schnepf@chemie.uni-karlsruhe.de; Fax: +49 (0)721 608 4854; Tel: +49 (0)721 608 2951*

**Andreas Schnepf**

*Andreas Schnepf received his PhD from the University of Karlsruhe in 2000 under the direction of Professor H. Schnöckel. From 2000 to 2002 he was a postdoctoral fellow at the Institute of Inorganic Chemistry at the University of Karlsruhe, where he worked with Prof. H. Schnöckel on physical properties of metalloid group 13 cluster compounds. During this period he completed research stays at the German Electron Synchrotron (DESY) in Hamburg and the Paul Scherrer Institute (PSI) in Villingen. From 2002 to 2006 he worked on his habilitation at the same institute and was appointed as Privatdozent in 2006. His current research interest is focused on the solution chemistry of metastable high-temperature group 14 metal halides and their use in the synthesis of metalloid group 14 cluster compounds.*

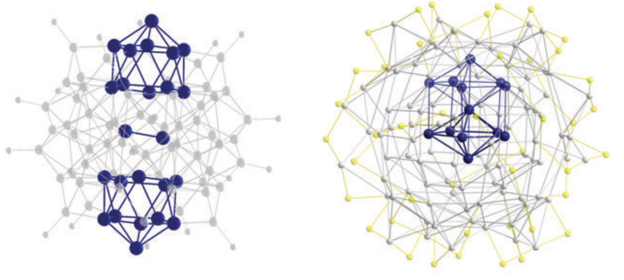

**Fig. 1** Molecular structure of the metalloid cluster compounds $Ga_{84}[N(SiMe_3)_2]_{20}^{4-}$ **10** (without $SiMe_3$ groups) and $Au_{102}[p\text{-MBA}]_{44}$ **11** (*p*-MBA = *p*-mercaptobenzoic acid; only the sulfur atom is shown). The central $Ga_2$ dumbbell and the icosahedral $Ga_{11}$ units are highlighted for **10**. The central $Au_7$ pentagonal bipyramid together with a bicapped pentagonal prism is highlighted for **11**.

thermodynamically stable structure of α-gallium. Additionally a structural resemblance to the low temperature phase δ-gallium is observed, as two nearly complete $Ga_{11}$ icosahedra are present (Fig. 1).[8] This unique feature also leads to unique physical properties as crystals exhibiting the tetraanion $Ga_{84}[N(SiMe_3)_2]_{20}^{4-}$ **10** are superconducting below 7 K,[9] while α-gallium exhibits a $T_c$ of only 1.1 K.[10]

A similar situation is found for the largest structurally characterized metalloid cluster compound of gold, $Au_{102}[p\text{-MBA}]_{44}$ **11** (*p*-MBA = *p*-mercaptobenzoic acid),[11] where first of all no central gold atom is found but a pentagonal bipyramidal $Au_7$ unit is present in the centre; an arrangement not known for elemental gold exhibiting a cubic close packed (ccp) structure. Nevertheless similar to elemental gold the coordination number for the inner gold atoms inside $Au_{102}[p\text{-MBA}]_{44}$ **11** is 12, but the coordination polyhedron of some of the central gold atoms is not a cuboctahedron, as found in a ccp structure but a bicapped pentagonal prism. For the other central gold atoms with coordination number 12 a strongly distorted cuboctahedron is observed. These examples show that the trivial suggestion that nanoscaled metal cluster compounds can be seen as a fragment of the solid state structure is not true even for clusters with diameters in the nanometre range—the diameter of the metal core is *ca.* 1.4 nm for **10** and **11**.

However somewhere in the nanometre regime such a structural transition must take place at least for germanium as *e.g.* the powder diffraction pattern of larger germanium nanoparticles (diameter more than 100 nm) are comparable to those of the bulk phase of α-germanium.[12]

As a consequence of the structural uncertainty in the case of metals or semi-metals, the structural characterization of metalloid cluster compounds is the first step to establish structure–property relations in the area between molecules and the solid state. However, obtaining structural information about these compounds is not trivial and many highly sophisticated methods have been established even for naked metal atom clusters in the gas phase, where the situation is less complicated due to an overall oxidation state of zero of the metal atoms; *e.g.* gas phase drift measurements or electron diffraction measurements together with quantum chemical calculations have been used to get structural information about small naked gold or tin clusters in the gas phase.[13]

Nevertheless, the best experimentally available structural information are from X-ray crystal structure analysis; but to obtain a crystalline compound a metalloid cluster has to be isolated in pure form, being quite complicated as metalloid cluster compounds are metastable intermediates on the way to the bulk phase as emphasized in Scheme 5. Thus special synthetic methods have been established, which are described in the following, after a short discussion of solid state structures of germanium.

### 1.1 Elemental structures of germanium

As metalloid cluster compounds of germanium can be seen as intermediates on the way from oxidized compounds to elemental germanium[14] it is reasonable to take first of all a short look into known solid state structures of germanium: elemental germanium normally crystallizes in a cubic diamond lattice (α-germanium, Ge(*cF*8)), where every germanium atom is tetrahedrally bound to four other germanium atoms with a Ge–Ge distance of 245 pm.[15] Additionally, several high-pressure modifications of germanium have been structurally characterized.[16] After pressure release the normal pressure modifications γ-Ge (Ge(*tP*12)) and δ-Ge (Ge(*cI*16)) have been obtained.[17,18] In both allotropes (γ- and δ-Ge) the germanium atoms are still fourfold coordinated but the bond angles deviate considerably from the ideal tetrahedral angle of 109.5°. γ-Ge crystallizes in a three dimensional arrangement with five and seven membered rings while δ-Ge comprises six-membered rings (Fig. 2).

In 2006 a novel element modification, Ge(*cF*136) was identified by Grin *et al.*,[19] which is obtained by the oxidation of the Zintl anion $Ge_9^{4-}$ by an ionic liquid.[20] In this novel modification all germanium atoms are again fourfold coordinated and are arranged in the clathrate(I) form. Hence, inside Ge(*cF*136) two different polyhedra are present: a pentagonal dodecahedron built up of 20 atoms and a hexakaidecahedron exhibiting 28 atoms (Fig. 2). Additionally, the reaction of the Zintl phase $Mg_2Ge$ with $GeCl_4$ yields "mesostructured germanium with cubic pores",[21] whereas the oxidation of the Zintl ion $(Ge_9^{2-})_n$ with ferrocenium hexafluorophosphate in

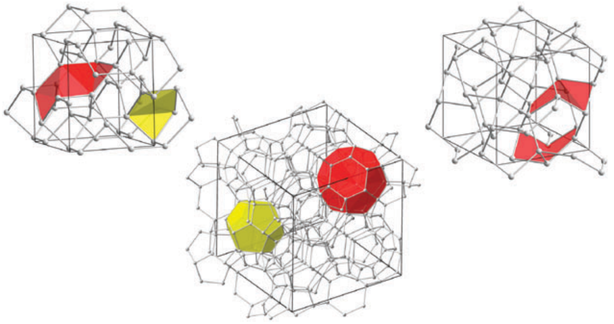

**Fig. 2** Section of the solid state structures of γ-germanium (left), δ-germanium (right) and Ge(*cF*136) (middle). The five- and seven-membered rings (γ-Ge) as well as the six-membered rings (δ-Ge) are highlighted *via* a polyhedral presentation. In the case of Ge(*cF*136) the $Ge_{20}$ pentagonal dodecahedron (bright) and the $Ge_{28}$ hexakaidecahedron (dark) are highlighted by a polyhedral presentation.

**Table 1** Tabulation of structurally characterized metalloid cluster compounds of germanium, sorted by the number of germanium atoms present in the cluster core (Ar = 2,6-DIPP$_2$–$C_6H_3$; DIPP = 2,6-*i*Pr$_2$–$C_6H_3$; R = CH(SiMe$_3$)$_2$)

| Molecular formulae | Number in the text | Literature |
|---|---|---|
| $Ge_5R_4$ | **1** | 25 |
| $Ge_6Ar_2$ | **2** | 26 |
| $Ge_8[N(SiMe_3)_2]_6$ | **3** | 27 |
| $Ge_8[C_6H_3\text{–}2,6\text{-}(OtBu)_2]_6$ | **4** | 28 |
| $\{Ge_9[Si(SiMe_3)_3]_3\}^-$ | **5** | 29 |
| $\{Ge_{10}(SitBu_3)_6I\}^+$ | **6** | 30 |
| $\{Ge_{10}Si[Si(SiMe_3)_3]_4(SiMe_3)_2Me\}^-$ | **7** | 31 |
| $Na_6(THF)_{12}Ge_{10}[Fe(CO)_4]_8$ | **8** | 32 |
| $Li_3(THF)_6Ge_{14}[Ge(SiMe_3)_3]_5$ | **9** | 33 |

the presence of a surfactant (cetyltriethylammonium bromide) led to "hexagonal nanoporous germanium".[22]

In addition to these structurally characterized modifications a great variety of nanosized germanium particles have been synthesized by a variety of methods, *e.g.* $H_2$ reduction of a mixed oxide ($Ge_xSi_{1-x}O_2$),[23] showing unusual physical properties; *e.g.* germanium nanoparticles exhibit a size-dependent photoluminescence[24] (PL) while elemental germanium does not show a comparable PL. For these nanoparticles no structural information is available so far, but the different physical property with respect to the bulk phase hints to a different structure and to establish a structure–property relation first of all the structure has to be determined. An experimental access to such information can be seen in the synthesis and structural characterization of metalloid cluster compounds of germanium as model compounds for this area between molecules and the solid state. Results obtained during recent years (Table 1) are discussed in the following.

## 2. Synthesis

As mentioned before, the synthesis of a metalloid cluster compound is not trivial as these compounds are metastable intermediates on the way to the bulk phase (elemental germanium) and therefore kinetic stabilization and low reaction temperatures are needed. As additionally oxidized species like $GeO_2$ are reduced only under drastic reaction conditions, a balanced reaction course is needed and to date three synthetic routes have been identified, where kinetic stabilization is provided by bulky ligands like $N(SiMe_3)_2$, $Si(SiMe_3)_3$ or $C_6H_3Dipp_2$ (Dipp = 2,6-*i*Pr$_2$–$C_6H_3$), shielding the germanium core. However, the synthesis of a definite metalloid cluster cannot be planned on a sheet of paper and only the framework (synthetic route) in which such a compound might form can be provided. In the following the basic principles of the various synthetic routes are discussed:

### (a) Reductive elimination route

The reductive elimination of a leaving group XY can lead to "naked"[34] germanium atoms when X and Y are the last ligands bound to the germanium atoms. If the number of germanium atoms in the product exceeds those of the remaining ligands one can get access to a metalloid cluster compound (Scheme 1).

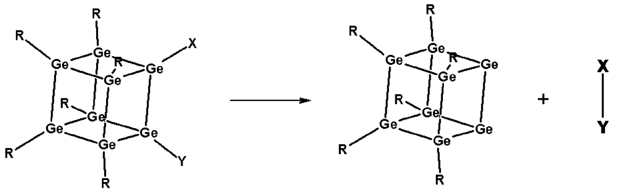

**Scheme 1** Schematic presentation of the synthetic route for the synthesis of a metalloid cluster *via* reductive elimination.

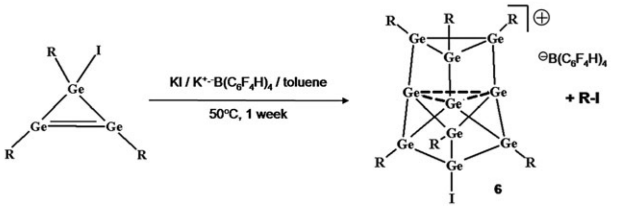

**Scheme 2** Reaction scheme for the synthesis of the metalloid cluster compound **6** (R = Si*t*Bu$_3$).

This synthetic route is suggested by Sekiguchi *et al.* for the synthesis of the cationic metalloid cluster compound $\{Ge_{10}(SitBu_3)_6I\}^+$ **6**,[30] which is synthesized *via* the reaction of the germacyclopropene $Ge_3(SitBu_3)_3I$ with a mixture of potassium salts ($KI/KB(C_6F_4H)_4$) at 50 °C in toluene over one week (Scheme 2). Thus the three naked germanium atoms in **6** are obtained *via* reductive elimination of I–Si*t*Bu$_3$, which was identified as a by-product in the reaction mixture by NMR spectroscopy. However the complete reaction sequence is not known but it can be assumed that a couple of different reactions must take place until a $Ge_{10}$ cluster is formed from a $Ge_3$ precursor. This drawback holds true for every metalloid cluster compound, all of which are obtained from precursors with only few germanium atoms. Nevertheless it must be one goal for the future to establish a deeper insight into this complicated reaction course, so that the synthesis of a metalloid cluster might be planned one day, maybe only roughly on a sheet of paper.

### (b) Reductive coupling route

When the reductive coupling of a germylene RGeX (R = bulky ligand; X = halide atom) is performed in the presence of a Ge(II) halide with a strong reducing agent like potassium, the Ge(II) halide like $GeCl_2$·dioxane might be reduced completely and incorporated inside the cluster core as naked germanium atoms (Scheme 3), leading to a metalloid cluster compound.

Hence this synthetic route can be seen as an enhancement of the reductive coupling reaction, used for the synthesis of

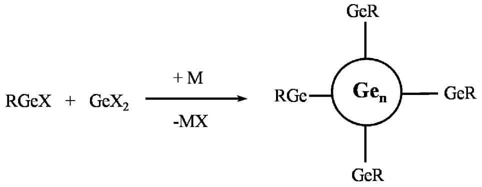

**Scheme 3** Schematic presentation of the synthesis of a metalloid cluster compound *via* the synthetic route of reductive coupling.

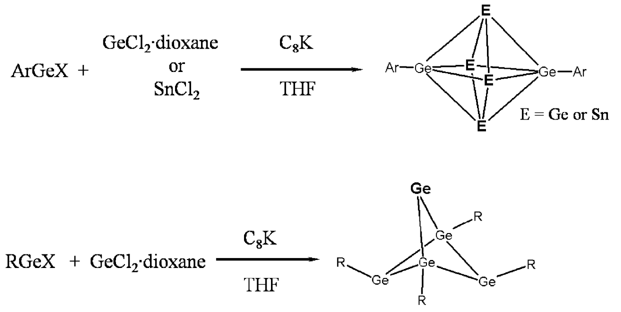

**Scheme 4** Reaction scheme for the synthesis of the metalloid cluster compound $Ge_6Ar_2$ **2** [$Ge_2Sn_4Ar_2$] (Ar = 2,6-Dipp$_2$–$C_6H_3$; Dipp = 2,6-*i*Pr$_2$–$C_6H_3$) and $Ge_5R_4$ **1** (R = 2,6-Mes$_2$–$C_6H_3$ (Mes = 2,4,6-Me$_3$–$C_6H_2$) or $CH(SiMe_3)_2$). The naked germanium atoms are highlighted by a bold presentation.

cluster compounds of the general formulae $Ge_nR_n$, where every germanium atom bears a ligand; *i.e.* tetrahedral $Ge_4R_4$ (R = Si*t*Bu$_3$),[35] trigonal prismatic $Ge_6R_6$ (R = $CH(SiMe_3)_2$)[36] and cubic $Ge_8R_8$ (R = 2,6-Et$_2$–$C_6H_3$).[37] As the synthesis of $Ge_nR_n$ clusters normally gives yields of 3–10%, a further complication should lead to lower yields and consequently one would not expect that this synthetic route could work.

However, the opposite is true as Power *et al.* were able to isolate the octahedral $Ge_6$ cluster $Ge_6Ar_2$ **2** (Ar = 2,6-DIPP$_2$–$C_6H_3$; DIPP = 2,6-*i*Pr$_2$–$C_6H_3$) by reductive coupling of the germylene ArGeCl in the presence of $GeCl_2$·dioxane with $C_8K$ in 40% yield.[26] Also the mixed metalloid cluster $Sn_4Ge_2Ar_2$ **2a** was obtained in 20% yield under the same reaction conditions when $SnCl_2$ is used instead of $GeCl_2$·dioxane. Additionally, when the organic ligand at the germylene is $CH(SiMe_3)_2$ or 2,6-Mes$_2$–$C_6H_3$ (Mes = 2,4,6-Me$_3$–$C_6H_2$) a metalloid $Ge_5R_4$ cluster **1** is formed in 20% yield,[25] where a naked germanium atom is bound to two germanium atoms of a butterfly $Ge_4R_4$ unit (Scheme 4).

### (c) Disproportionation reaction

As metalloid cluster compounds can be seen as intermediates on the way to the elemental state (Scheme 5) the best way to obtain such compounds might be during element formation. However elemental germanium is synthesized by the reduction of $GeO_2$ with elemental hydrogen at 650 °C[15] and under these drastic reaction conditions metalloid cluster compounds can rather be obtained in reasonable yields on the way to elemental germanium.

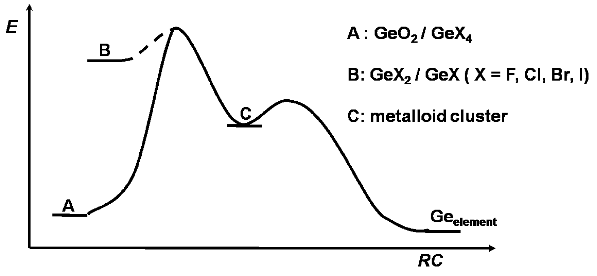

**Scheme 5** Schematic development of the energy during the synthesis of elemental germanium from oxidized starting materials.

Thus a different starting material is necessary that reacts more easily to the elemental state at lower reaction temperatures (B in Scheme 5) and in recent years it turned out that subhalides are ideal candidates for such a reaction course, as the disproportionation reaction takes place under milder reaction conditions. However the well known Ge(II) halides are not suitable starting materials as for example $GeBr_2$ only disproportionates at temperatures higher than 150 °C which is still a temperature too high for a kinetic stabilization of intermediates on the way to the bulk phase. Nevertheless monohalides of germanium obtained *via* a preparative co-condensation technique[38] disproportionate at lower reaction temperatures (solid GeBr at 90 °C) and are therefore better starting materials. However, for the synthesis of the high temperature molecule GeBr in preparative scale, the special synthetic technique of the preparative co-condensation has to be applied.[39] Hence, the co-condensation apparatus shown in Fig. 3 has to be used, where elemental germanium is reacted with HBr at 1600 °C and where the resulting gas particles are condensed together with a solvent mixture at −197 °C.

After the co-condensation reaction is finished the solid matrix is heated to *e.g.* −78 °C where the solvent melts, leading to a metastable solution of GeBr. When this solution is further heated, the monohalide starts disproportionation, leading in the end to the thermodynamically stable products elemental germanium and $GeBr_4$. In the course of this disproportionation reaction germanium rich clusters are formed on the way to the elemental state exhibiting halide substituents bound to the surface germanium atoms (Scheme 6).

These halide atoms can be substituted by bulky ligands in a subsequent metatheses reaction. Through this substitution the germanium core is then shielded by a ligand shell and therefore this cluster is now kinetically stabilized and can be isolated. This principle synthetic route, leading from a monohalide in

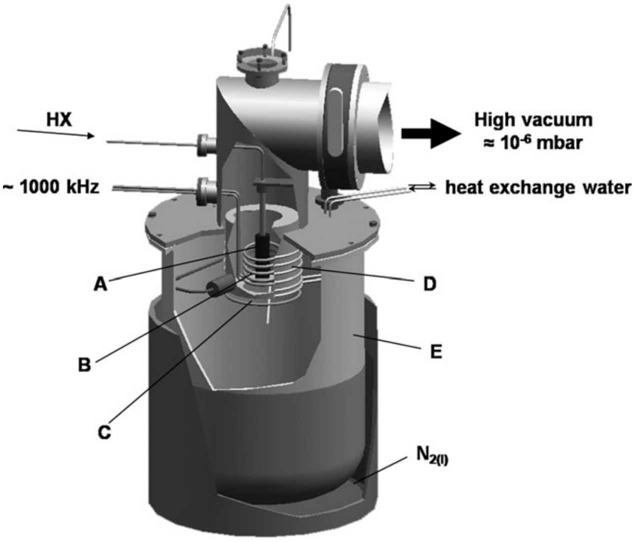

**Fig. 3** Scheme of the co-condensation apparatus for the synthesis of Ge(I) halides: A = graphite reactor; B = induction coil; C = solvent inlet; D = copper cooling shield; E = stainless steel vessel (≈30 l); HX = hydrogen halide gas.

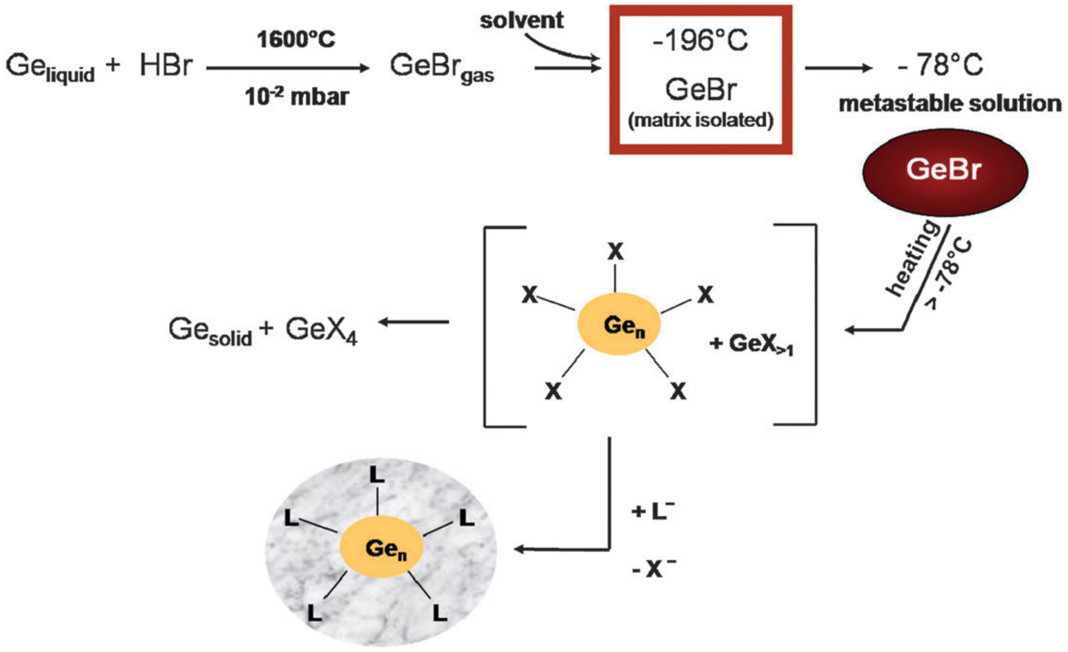

**Scheme 6** Schematic presentation of the synthesis of a metalloid cluster compound *via* synthetic route c, applying the disproportionation reaction of a monohalide (lower part), together with the schematic presentation of the preparative co-condensation technique (upper part).

the gas phase to a metalloid cluster compound in solution, is emphasized in Scheme 6.

This synthetic strategy can lead to giant cluster compounds as it takes advantage of the intrinsic property of a subhalide whose disproportionation reaction leads in the end to the element itself. For the heavier elements of group 13, aluminium and gallium, this was shown by Schnöckel *et al.*, who were able to synthesize cluster compounds with up to 77 aluminium[40] or 84 gallium atoms[7] in the cluster core. Thus this strategy can lead to metalloid cluster compounds with diameters in the nanometre range, when the right reaction conditions are known. And exactly this point is the major problem to be solved during the synthesis of a metalloid cluster compound as no definite synthetic protocol is known and therefore for every reaction system many experiments are necessary until the right reaction conditions are established. Hence the disproportionation reaction definitively leads to metalloid cluster compounds, but finding the right reaction conditions under which these compounds are formed and simultaneously stabilized by a ligand shell is very difficult.

Nevertheless this synthetic route proved to be quite successful for germanium as from the nine structurally characterized metalloid clusters known so far (Table 1), six are synthesized *via* the synthetic route applying the disproportionation reaction of a Ge(I) halide. However a mixture of several routes a–c may be involved in the complicate formation of a metalloid cluster from small precursors with only a few germanium atoms. This becomes apparent first of all by the synthesis of the metalloid Ge$_9$ cluster $\{Ge_9[Si(SiMe_3)_3]_3\}^-$ **5** that is synthesized by the reaction of GeBr with LiSi(SiMe$_3$)$_3$ (route c) and is isolated in 40% yield. This high yield is quite unusual with respect to such a complicated reaction course but was an important prerequisite for subsequent reactions with metalloid cluster compounds.[41] During the synthesis of **5**, the molecular compound (SiMe$_3$)$_3$Si–Si(SiMe$_3$)$_3$ could be identified as a by-product in the reaction mixture. One possible source of this by-product is the reductive elimination of R$_2$ from a germanium cluster core as discussed for synthetic route a (*vide supra*):

$$Ge_xR_y \rightarrow Ge_xR_{y-2} + R\text{–}R$$

However, with respect to the large steric bulk of the Si(SiMe$_3$)$_3$ ligand such a possibility seems quite unusual as the transition state of this reductive elimination is extremely crowded. In the course of the formation of the cationic cluster $\{Ge_{10}(Si\textit{t}Bu_3)_6I\}^+$ **6** the less crowded compound I–Si*t*Bu$_3$ is eliminated. Nevertheless gas phase measurements on $\{Ge_9[Si(SiMe_3)_3]_3\}^-$ **5** indicate that such a process is energetically favourable;[42] *i.e.* collision induced dissociation experiments show that $\{Ge_9[Si(SiMe_3)_3]_3\}^-$ **5** dissociates in the gas phase first of all by the elimination of (SiMe$_3$)$_3$Si–Si(SiMe$_3$)$_3$ (**5** → **5a**) and not by the consecutive elimination of two Si(SiMe$_3$)$_3$ radicals.[43] Afterwards, the elimination of the third ligand occurs on different routes depending on the method applied. These different fragmentation channels occur as there exists an activated isomerization (**5a** → **5b**) that leads to different final products (**5d** and **5e**) if an "off"- or "on"-resonant excitation is applied (Scheme 7).

The gas phase measurements together with the identification of (SiMe$_3$)$_3$Si–Si(SiMe$_3$)$_3$ in the reaction mixture clearly show that the formation of $\{Ge_9[Si(SiMe_3)_3]_3\}^-$ **5** not only proceeds *via* disproportionation of the subhalide but also by reductive elimination of R$_2$ from a Ge$_9$R$_{3+x}$ cluster, which seems to be quite effective as **5** is isolated in rather high yields. Hence for the first time an insight is given on the reaction course indicating that the situation is more complicated as emphasized by the simple picture shown in Scheme 6.

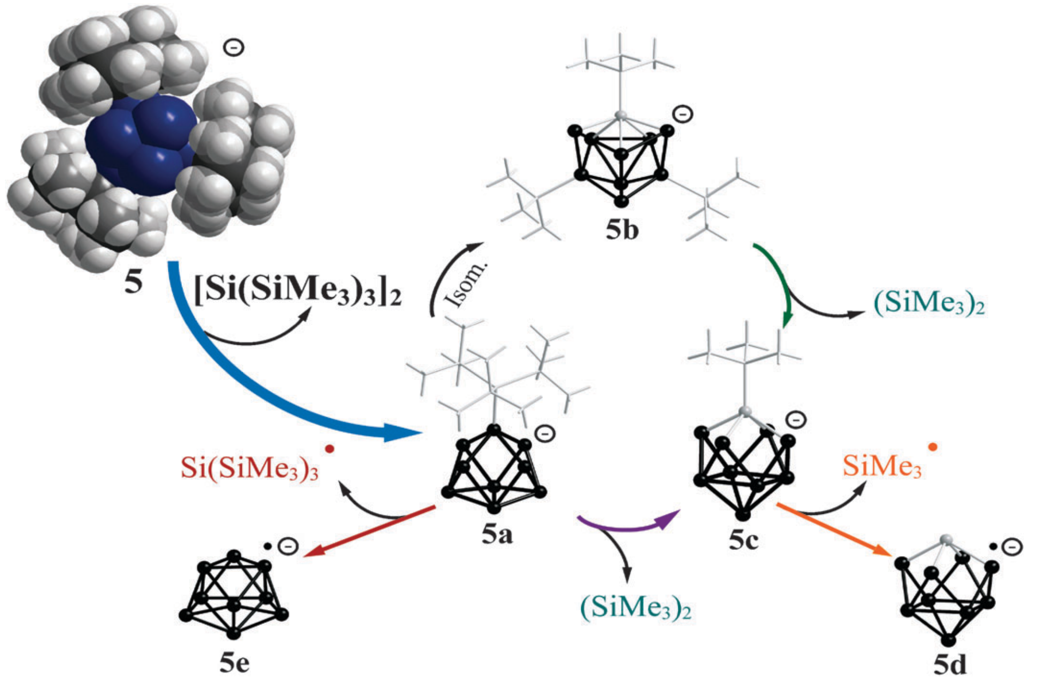

**Scheme 7** Schematic presentation of the dissociation behavior of $\{Ge_9[Si(SiMe_3)_3]_3\}^-$ **5** (space filling model top left) after gas phase collision.

## 3. Structural and bonding properties of metalloid clusters

As the most important issue of metalloid clusters of germanium is the model character for the area between molecules and the bulk phase of elemental germanium their structures and electronic properties will be discussed with respect to the size of the cluster and average oxidation state of the germanium atoms inside the cluster.

Compared to the fully substituted cluster compounds of the general formulae $Ge_nR_n$ ($n$ = 4, 6, 8) metalloid clusters exhibit in addition to ligand bound germanium atoms also naked germanium atoms that exclusively form germanium–germanium bonds. Thus in a gedankenexperiment the elimination of two ligands R from the cubic cluster $Ge_8R_8$ would lead to a metalloid cluster of the formulae $Ge_8R_6$. This metalloid cluster could also be achieved by the addition of two germanium atoms to the trigonal prismatic $Ge_6R_6$ cluster (Scheme 8). Hence, the question arises what happens to the bonding situation inside a ligand stabilized cluster when additional electrons and/or naked atoms are added; *i.e.* what happens to the remaining electron on homolytic cleaving the 2c2e bond to a ligand.

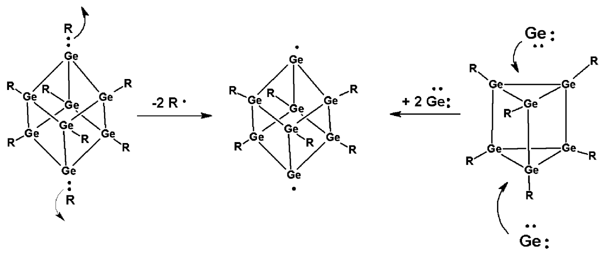

**Scheme 8** Schematic presentation of the formation of a metalloid cluster compound from a fully substituted cluster by ligand elimination or addition of naked germanium atoms.

This question could be addressed by the metalloid cluster $Ge_8[N(SiMe_3)_2]_6$ **3** which could be synthesized by the reaction of a metastable GeBr solution with $LiN(SiMe_3)_2$ (method c). The arrangement of the germanium atoms inside the cluster core of **3** is best described as distorted cubic as two different Ge–Ge distances of 250 (Ge–GeR) and 267 pm (GeR–GeR) are found inside the cluster core. The naked germanium atoms are at opposite sides of the cube with a non-bonding Ge–Ge distance of 517.5 pm.

Comparing the bond distances in **3** with those found in the fully substituted cubic $Ge_8R_8$ cluster (R = 2,6-$Et_2$–$C_6H_3$),[37] where Ge–Ge distances of 249 pm are found, shows that the elimination of ligands leads to an elongation of Ge–Ge bond distances. This observation seems unusual at first sight as one would expect a shortening of bond distances as now two extra electrons from the naked germanium atoms are available for cluster bonding leading to multiple bonding.

However the formation of multiple bonds seems to be unfavorable for metalloid cluster compounds of germanium as there is no example known to date where a multiple bond is formed.[44] Quite contrary the bond order of the remaining Ge–Ge bonds shrinks as the bond distance increases. The decrease of the bond order is corroborated by quantum chemical calculations on the model compound $Ge_8(NH_2)_6$ **3a** where the *shared electron number* (SEN) of the two centre bonding components is only 0.88 for the long RGe–GeR bond of 267 pm. In comparison, the SEN of the two centre bonding component of a classical two centre two electron bond is 1.04 for the model compound $(NH_2)_3Ge$–$Ge(NH_2)_3$.

In addition to the two centre bonding components inside **3a** also three centre bonding components are present in the cluster core with a SEN of 0.13 in the three-membered ring of ligand bound germanium atoms, *i.e.* the presence of the

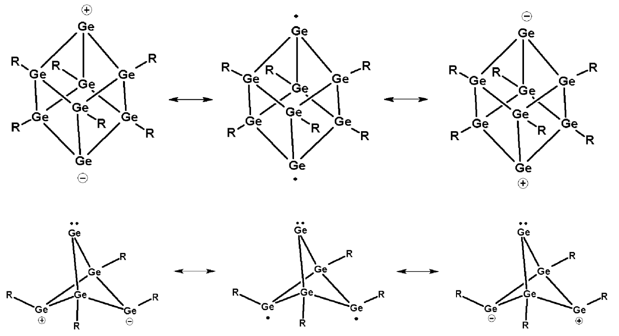

**Scheme 9** Possible resonance forms for the presentation of the bonding situation in $Ge_8[N(SiMe_3)_2]_6$ **3** and $Ge_5R_4$ **1** (R = $CH(SiMe_3)_2$).

extra electrons leads to a delocalization of bonding electrons inside the cluster core.

However, in a more classical view the bonding situation in **3** might be described by the three resonance forms depicted in Scheme 9, which is similar to the description of the bonding in the smallest metalloid cluster of germanium $Ge_5R_4$ **1**.[25] Thereby the ionic structure is only favorable for the anionic part ($Ge^-$). For the cationic part ($Ge^+$) the arrangement is energetically unfavorable as a germyl cation should exhibit a planar structure as it was recently shown for the free germyl cations $R_3Ge^+$ (R = Si*t*Bu$_3$;[45] R = 2,6-(O*t*Bu)$_2$–$C_6H_3$[46]). The triplet biradical form could also be ruled out as on the one hand no *electron paramagnetic resonance* (EPR) signal is observed for **3** and on the other hand the singlet state is the ground state due to quantum chemical calculations on **3a**.

However the triplet state is only 96.5 kJ mol$^{-1}$ higher in energy for the model compound $Ge_8[NH_2]_6$ **3a** being in the range normally calculated for singlet biradicaloids.[47] Consequently **3** might be a member of the growing group of singlet biradicaloid compounds of group 14, which might be clarified by future theoretical and experimental investigations.

As metalloid clusters are ligand protected molecular compounds, the influence of the ligand on the bonding and physical properties is also an important aspect. This subject area could be addressed experimentally by the isolation of a second metalloid cluster of the formulae $Ge_8R_6$, where aryl ligands ($C_6H_3$(O*t*Bu)$_2$) bind to the germanium atoms. In the case of $Ge_8[C_6H_3(OtBu)_2]_6$ **4** the eight germanium atoms inside the cluster core are arranged nearly perfectly cubic (Ge–GeR: 252 pm; GeR–GeR: 250 pm), indicating that the bonding electrons are now more localized as the Ge–Ge distances are now nearly comparable to those found in the cubic $Ge_8R_8$ compound. This situation was also confirmed by quantum chemical calculations on different $Ge_8R_6$ model compounds that indicate that a ligand exhibiting a lone pair at the atom directly bound to the germanium atom leads to stronger delocalization of bonding electrons inside the cluster core.[46]

The different bonding situation also leads to different physical properties which is best seen from the color of the crystals (Fig. 4); thus while crystals of the aryl substituted cluster **4** are orange red those of the amide substituted **3** are nearly black. This result clearly shows that the ligand can have an important influence on the physical property of a metalloid cluster and thus maybe of a nanoparticle, which is important for nanotechnology as it shows that the physical property of a nanoparticle might not only be changed by the size of the particle but also by the ligand (surfactant) applied, which might be changed more easily.

Another fact that strongly influences the bonding situation in a metalloid cluster compound is the average oxidation state of the germanium atoms inside the cluster core. This area was first addressed by the metalloid cluster compounds $Ge_6Ar_2$ **2** (Ar = $C_6H_3Dipp_2$; Dipp = $C_6H_3$–2,6-*i*Pr$_2$) and $\{Ge_9[Si(SiMe_3)_3]_3\}^-$ **5** (Fig. 5), where 4 and 6 naked germanium atoms are present, respectively, leading to an average oxidation state of the germanium atoms of 0.33 (**2**) and 0.22 (**5**). The two metalloid cluster compounds **2** and **5** are synthesized by different synthetic strategies. While $Ge_6Ar_2$ **2** was synthesized *via* a reductive coupling reaction of ArGeCl with $C_8K$ in the presence of $GeCl_2$ (route b; Scheme 3); the anionic compound $\{Ge_9[Si(SiMe_3)_3]_3\}^-$ **5** was synthesized from GeBr using $LiSi(SiMe_3)_3$ as the ligand source (route a/c; Scheme 1/6; *vide supra*). Both compounds exhibit highly symmetric arrangements of the germanium atoms inside the cluster core. The six germanium atoms in **2** are arranged octahedrally and the nine germanium atoms of **5** are arranged in the form of a tricapped trigonal prism (Fig. 5).

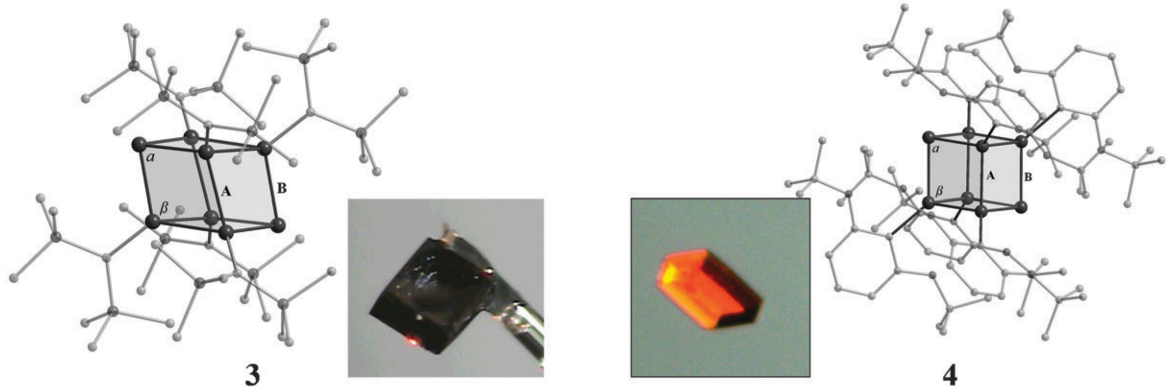

**Fig. 4** Molecular structure of the metalloid cluster compounds $Ge_8[N(SiMe_3)_2]_6$ **3** (left) and $Ge_8[C_6H_3(OtBu)_2]_6$ **4** (right) without hydrogen atoms. The central $Ge_8$ core is highlighted by a polyhedral presentation. **3**: *A* = 267 pm, *B* = 250 pm, *α* = 82°, *β* = 101°; **4**: *A* = 251 pm, *B* = 249 pm, *α* = 87°, *β* = 92°; central: photo of crystals of the cluster compounds $Ge_8[N(SiMe_3)_2]_6$ **3** (left) and $Ge_8[C_6H_3(OtBu)_2]_6$ **4** (right).

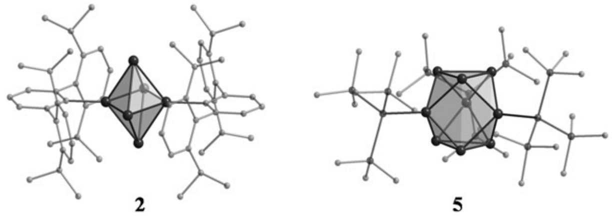

2 5

**Fig. 5** Molecular structure of the metalloid germanium cluster compounds $Ge_6Ar_2$ **2** (Ar = $C_6H_3Dipp_2$; Dipp = $C_6H_3$–2,6-*i*$Pr_2$) and $\{Ge_9[Si(SiMe_3)_3]_3\}^-$ **5** without hydrogen atoms. The arrangement of the germanium atoms in the cluster core is highlighted by a polyhedral presentation.

In both compounds two different germanium–germanium distances are found, following the same trend. Thus the germanium–germanium distance between ligand bound and naked germanium atoms amounts to 250 pm in **2** and 252 pm in **5**, while the germanium–germanium distances between naked germanium atoms are with 286 pm in **2** and 267 pm in **5** substantially longer. Quantum chemical calculations on the model compounds $Ge_6H_2$ **2′** and $Ge_9H_3^-$ **5′** reveal that in both compounds highly delocalized bonding electrons are present as the maximum SEN's of the three centre bonding components amount to 0.23 and 0.32 for **2′** and **5′** respectively.[48–50]

Thus, taking a closer look into the amount of delocalization of bonding electrons inside a metalloid cluster compound shows that the level of delocalization—indicated by the magnitude of the SEN of the multicenter bonding component—increases when the average oxidation state of the germanium atoms decreases as emphasized in Scheme 10. If this trend goes further on it would lead to elemental germanium (oxidation state = zero), with highly delocalized bonding electrons, representing a metallic state. Thus here an access to a metallic form of germanium seems possible and for the heavier element tin, the synthesis of a $Sn_{15}R_6$ compound (R = N[SiMe$_3$]Dipp; Dipp = $C_6H_3$–2,6-*i*$Pr_2$) shows that a metallic arrangement can be realized within metalloid group 14 cluster compounds.[51] Inside the $Sn_{15}$ compound the tin atoms are arranged in the form of a body-centered cubic (bcc) structure leading to a coordination number of 8 + 6 for the central tin atom.

However, a metallic state is quite unusual for the semi-metal germanium comprising a band gap of 0.6 eV. Hence, one would expect that at a larger size the trend of delocalization will invert leading to an elemental state with localized 2c2e bonds exhibiting a lattice with fourfold coordinated germanium atoms as in α-germanium (diamond lattice) or Ge(*cF*136) (clathrate(I) lattice).

Recent results indicate that such a transition might already occur at a size of ten germanium atoms in the cluster core. Thus the arrangement of the ten germanium atoms in the cluster core of the two metalloid $Ge_{10}$ cluster compounds $[Ge_{10}(Si\textit{t}Bu_3)_6I]^+$ **6** and $\{Ge_{10}Si[Si(SiMe_3)_3]_4(SiMe_3)_2Me\}^-$ **7** are very similar as can be seen in Fig. 6. This similarity is unusual, as there are significant differences between the compounds: firstly the average oxidation state of the germanium atoms inside the cluster core is 0.8 in the case of the cation **6** and 0.4 in the case of the anion **7**. Secondly one compound is a cation while the other compound is an anionic one and thirdly, and most important, the ligands in both cluster compounds are bound to different germanium atoms; *i.e.* as shown in Fig. 6, in the cation **6** Ge1 is bound to a ligand while Ge2 is naked and in the case of the anion **7** Ge1 is naked and Ge2 binds a ligand.

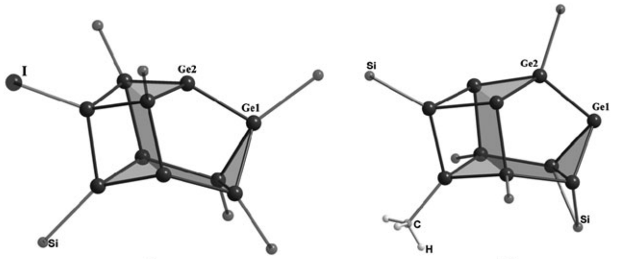

6 7

**Fig. 6** Molecular structure of $[Ge_{10}(Si\textit{t}Bu_3)_6I]^+$ **6** (left) and $\{Ge_{10}Si[Si(SiMe_3)_3]_4(SiMe_3)_2Me\}^-$ **7** (right) without $SiMe_3$ groups. The adamantane like arrangement of the germanium atoms inside the cluster core is emphasized by a polyhedral presentation.

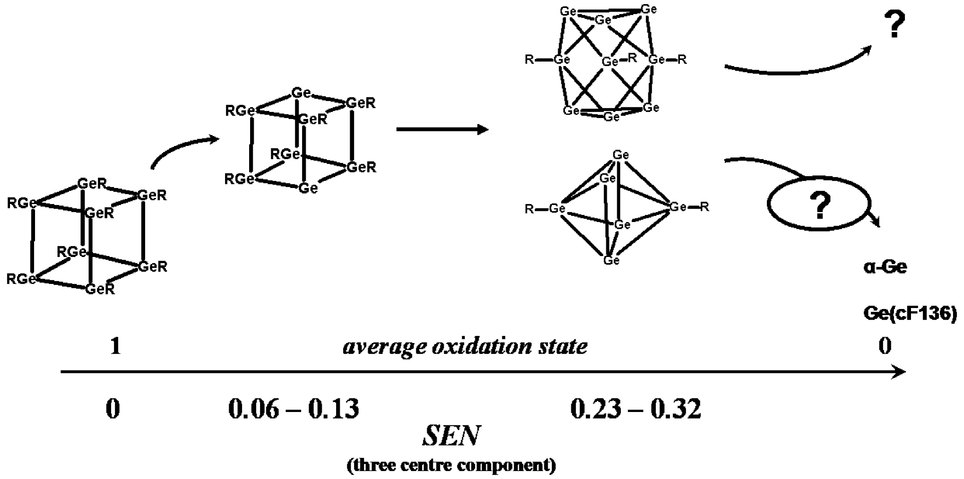

**Scheme 10** Comparison of the average oxidation state of the germanium atoms inside a metalloid cluster compound with the degree of delocalization of bonding electrons inside the cluster core.

The fact that besides all these differences the germanium atoms inside both compounds are arranged in a similar way shows that this arrangement is favourable for a metalloid cluster compound with 10 germanium atoms in the cluster core. A reason for this preference can be seen in the fact that in both compounds **6** and **7** an adamantane like arrangement of the 10 germanium atoms is present, as emphasized in Fig. 6 by a polyhedral presentation. Hence, for the first time a topological approach onto α-germanium is realized, which is much more pronounced in the case of the anionic compound **7**, as here the average oxidation state of the germanium atoms is with 0.4 much closer to the value 0 of the element.[52]

However, such a structural transition does not necessarily occur when ten germanium atoms are present inside the cluster core. This becomes obvious when the metalloid cluster compound $(THF)_{18}Na_6Ge_{10}[Fe(CO)_4]_8$ **8**, synthesized by the reaction of a GeBr solution with Collmann's reagent $Na_2Fe(CO)_4$ (method c), is taken into account.[32]

The arrangement of the ten germanium atoms in the cluster core of **8** is totally different from that of the two other $Ge_{10}$ compounds **6** and **7**. Hence, the 10 germanium atoms in **8** are arranged in a unique fashion. The polyhedron built up of the 10 germanium atoms in **8** exhibits two different sites and is built up of a cubic part on the one side and an icosahedron part on the other side as emphasized in Fig. 7. In accordance to the description of the *Centaur* of the Greek mythology (half human half horse), a polyhedron built of two different polyhedra (here: half cube half icosahedron) was named a centaur polyhedron[53] and therefore the polyhedron built up of the 10 germanium atoms in **8** can be named a centaur polyhedron. The centaur polyhedron is well known in solid state chemistry as it represents one possibility for coordination number 10. However, in **8** the centaur polyhedron is empty as no atom is localized inside the $Ge_{10}$ polyhedron, representing a novel structural motif in germanium chemistry.

Eight of the ten germanium atoms inside the cluster core of **8** are bound to one $Fe(CO)_4$ ligand each and the $Fe(CO)_4$ ligands are bound *via* the CO molecules to six sodium cations, which surround the cluster core in a pseudo octahedral fashion. The sodium cations are coordinatively saturated by three THF molecules each, leading to the neutral compound $(THF)_{18}Na_6Ge_{10}[Fe(CO)_4]_8$ **8**, which can be dissolved and recrystallized from THF. A closer look into the bonding situation inside the cluster core with the aid of quantum chemical calculations on the model compound $[Ge_{10}[Fe(CO)_4]_8]^{6-}$ **8′** reveals that inside the different sides of the centaur polyhedron also different bonding situations are present (Fig. 8).

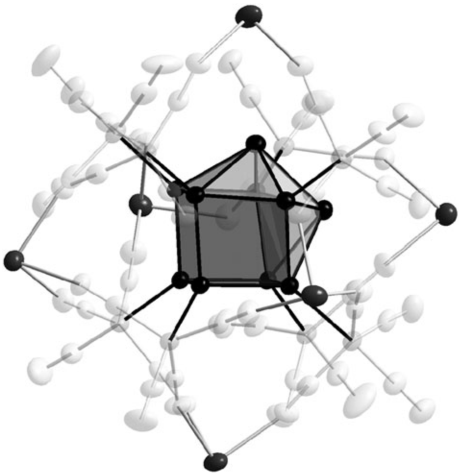

**Fig. 7** Molecular structure of $(THF)_{18}Na_6Ge_{10}[Fe(CO)_4]_8$ **8** without coordinating THF molecules. The central germanium atoms and the surrounding sodium atoms are dark colored. The different parts of the centaur polyhedron are highlighted by a polyhedral presentation where the cubic part is dark and the icosahedral part is bright.

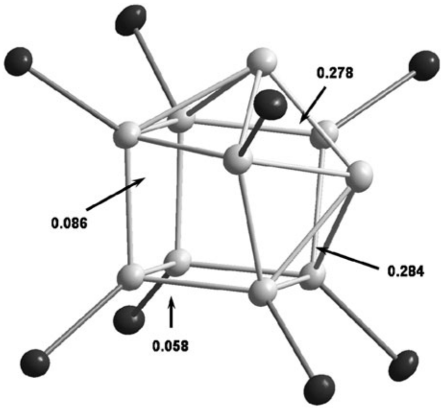

**Fig. 8** $Ge_{10}Fe_8$ core of the calculated model compound $[Ge_{10}[Fe(CO)_4]_8]^{6-}$. The calculated SEN's of the three centre bonding components are shown.

At the cubic side three centre bonding components with SEN's of 0.058 to 0.086 were calculated while the SEN's in the icosahedral part are in the range of 0.278 to 0.284. Thus the bonding situation inside **8′** can be described as that it changes from localized in the cubic part to delocalized in the icosahedral part of the centaur polyhedron. Such a bonding situation is hereby unique in the field of metalloid cluster compounds as, for example, in the large multi-shell metalloid cluster compounds of group 13,[54] the bonding situation changes from the inner to the outer side but not from one side to the other.

The unusual structure of **8** made a classification quite complicated and it seems as if this structural unit (centaur polyhedron) is an abnormal singular result. However this is not the case as only recently a comparable structure was observed in the metalloid cluster compound of tin $Sn_{10}[Si(SiMe_3)_3]_6$ $\mathbf{8_{Sn}}$, where the ten tin atoms are arranged in the form of a centaur polyhedron too.[55] Considering bond distances, electronic situation and Sn Mößbauer spectroscopy of $\mathbf{8_{Sn}}$, a correlation to a phase transition becomes obvious; *i.e.* the change of bond distances as well as electronic properties from the cubic (localized bonding electrons, short Sn–Sn bonds) to the icosahedral part of the centaur polyhedron (delocalized bonding electrons, long Sn–Sn distances) can be correlated to the phase transition from α- to β-tin.

This correlation only becomes obvious for $\mathbf{8_{Sn}}$ as α- and β-tin are stable at normal conditions with a phase transition temperature of 13.2 °C.[15] In the case of germanium, β-germanium is a high pressure modification leading to shorter Ge–Ge distances.[56] However, the calculated atomic volumes, obtained like those for tin,[57] show that in the case of germanium the atomic volume also shrinks by 11% (12% in the case of $\mathbf{8_{Sn}}$) on

**Table 2** Calculated atomic volumes [Å$^3$] of germanium atoms in $(THF)_{18}Na_6Ge_{10}[Fe(CO)_4]_8$ **8** and in an adamantane cut-out of α-germanium

| | |
|---|---|
| $(THF)_{18}Na_6Ge_{10}[Fe(CO)_4]_8$ | 32.564 |
| $Ge_{10}$-section (adamantane unit) of α-germanium | 36.787 |

going from adamantine $Ge_{10}$ as in α-germanium to the $Ge_{10}$ centaur polyhedral arrangement in **8** (Table 2).

Consequently, the centaur polyhedral arrangement of the ten germanium atoms in **8** also hints to a phase transition from α- to β-germanium on going from the cubic to the icosahedral part of the centaur polyhedron, although in the case of germanium, β-germanium is only stable at a pressure above 11 GPa.[56] However, metal atom arrangements of high pressure modifications inside a metalloid cluster compound, stable at normal conditions, are frequently observed in metalloid clusters, indicating that the ligand shell might induce a higher "pressure" in the cluster core.[58] Nevertheless also more open structures are possible as seen in the largest structurally characterized metalloid cluster compound of germanium $Li_3(THF)_6Ge_{14}[Ge(SiMe_3)_3]_5$ **9** (Fig. 9)[33] synthesized by the reaction of GeBr with $LiGe(SiMe_3)_3$ (route c). In **9** only five out of the 14 germanium atoms of the cluster core are bound to a $Ge(SiMe_3)_3$ ligand with an average Ge–Ge bond distance of 248 pm, being in a normal range for a Ge–Ge single bond. Additionally, three germanium atoms are coordinated to a lithium cation, which is additionally saturated by two THF molecules each. Thus the coordination number of the lithium cation is only three, leading to quite short Li–O distances of 188.9 pm.[59] The five ligands together with the THF molecules completely shield the cluster core of 14 germanium atoms as seen in the space filling model shown in Fig. 9.

The 14 germanium atoms inside the cluster core are arranged in a unique way, not known before in germanium chemistry. Most noteworthy is the fact that they comprise an empty polyhedron that is not spherical—but discus-like, as the shortest Ge–Ge distance between opposite germanium atoms is 411 pm and the longest is 658 pm (Fig. 10). The polyhedron is built up of six five-membered rings and three four-membered rings that are distorted to a butterfly arrangement leading to a diagonal Ge–Ge contact of 285.6 pm. The other Ge–Ge distances inside **8** are in a short range between 246 and 256 pm, which is in the range for a normal Ge–Ge single bond. This description is further corroborated by quantum chemical calculations that hint to classical 2c2e bonds for these short bonds as the SENs for the two centre bonding components are nearby those found for a normal Ge–Ge single bond. Thus inside **9** four kinds of differently bound germanium atoms are present (Fig. 10).

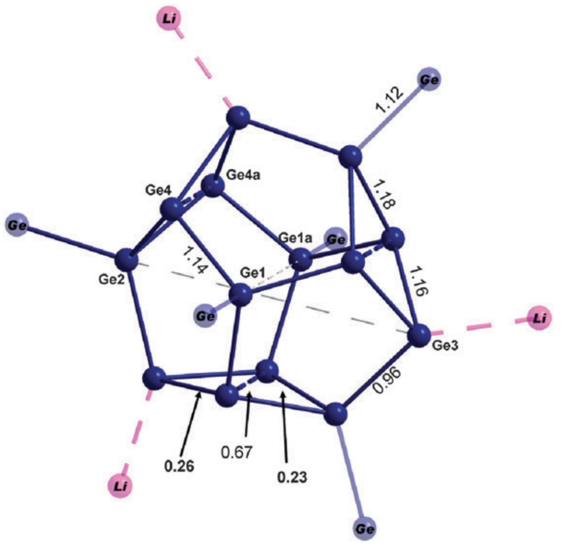

**Fig. 10** Arrangement of the 14 germanium atoms in $Li_3(THF)_6Ge_{14}$-$[Ge(SiMe_3)_3]_5$ **9** without $SiMe_3$ groups and THF molecules. Calculated SENs for the two- and three-centre bonding components are shown, where the three-centre SENs are bold (*d*(Ge1–Ge1a): 411 pm; *d*(Ge2–Ge3): 658 pm).

For the central germanium atom (Ge1) a classical bonding situation is observed with four tetrahedrally arranged bonding partners. For the other ligand bound germanium atom (Ge2)

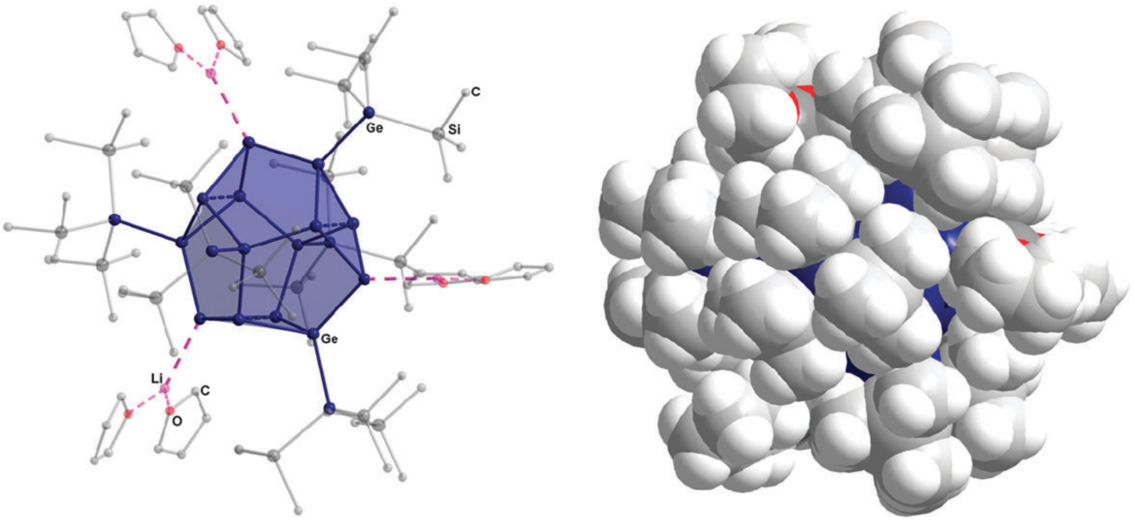

**Fig. 9** Left: molecular structure of the metalloid germanium cluster compounds $Li_3(THF)_6Ge_{14}[Ge(SiMe_3)_3]_5$ **9** without hydrogen atoms. The arrangement of the central 14 germanium atoms is highlighted by a polyhedral presentation. Right: space filling model of **9**.

as well as the lithium coordinated germanium atom (Ge3) a classical bonding situation with four nearly tetrahedrally bound substituents is present too. In the case of the naked germanium atoms (Ge4, Ge4a) the situation is different, as here, first of all only three bond distances are in the range of a normal Ge–Ge single bond of 245 pm; the fourth Ge–Ge contact (Ge4–Ge4a) is strongly elongated to 285.6 pm. Additionally the four bonding partners are not arranged tetrahedrally.[60] The arrangement resembles more the situation found *e.g.* in the propellanes[61] and only further theoretical investigations will show if **9** is a member of the group of biradicaloids.[47]

Due to the non-classical bonding situation of the naked germanium atoms again multi-centre bonding components are calculated for **9**. Thus the SEN for the three-centre bonding component in the three-membered rings comprising the naked germanium atoms and the ligand bound or lithium coordinated germanium atoms is 0.23 and 0.26 respectively (Fig. 10).

As mentioned before the arrangement of the 14 germanium atoms in **9** is unique in the field of molecular compounds but it is comparable to a lately described $Sn_{14}$ polyhedron in the Zintl phase $Na_{29}Zn_{24}Sn_{32}$ (Fig. 11).[62] However there are significant differences: (a) the $Sn_{14}$ polyhedron exhibits planar four-membered rings leading to a spherical arrangement; (b) the $Sn_{14}$ polyhedron is not empty as a sodium cation is present in the centre and (c) the $Sn_{14}$ polyhedron is a section of a solid state structure, thus the $Sn_{14}$ polyhedra are embedded in the matrix of the other atoms, leading to a linear arrangement of $Sn_{14}$ polyhedra with an *exo* tin–tin contact of 288 pm. Nevertheless the fact that a similar arrangement is realized in a molecular compound as well as in a solid state compound shows that such a polyhedron is a stable structural motif in group-14 chemistry. Additionally the fact that in the case of **9** an empty polyhedron is realized shows that even the heavier congeners of carbon can build up larger empty polyhedra without a stabilizing atom in the centre. Consequently also fullerene-like compounds might be accessible and **9** can be seen as a first step into this direction.

However another interpretation became obvious only recently when the novel solid state structure of germanium, Ge(*cF*136), was developed. The germanium atoms in Ge(*cF*136) are arranged in a clathrate(I) form (*vide supra*). Hence Ge(*cF*136) exhibits the sub-structural motif of a pentagon dodecahedron and a hexacaidecahedron. In both polyhedra the structural motif of three directly bound five-membered rings are present, which is also a central structural motif of **9** (Fig. 12). Consequently, as the arrangement of the germanium atoms in the adamantine unit of **6** and **7** could be seen as a structural approach to α-germanium, the arrangement of the germanium atoms in **9** can be seen as a structural approach onto the solid state structure of Ge(*cF*136) or maybe another clathrate-like arrangement.

Which interpretation fits best has to be clarified by future experiments and theoretical calculations giving more insight on the area between the molecular and the solid state. However, the results obtained so far show that, although germanium exhibits only few solid state structures, a complicated situation is present in the area between molecules and the solid state, where also fullerene-like compounds might be present and where a great variety of structural motifs emerge.

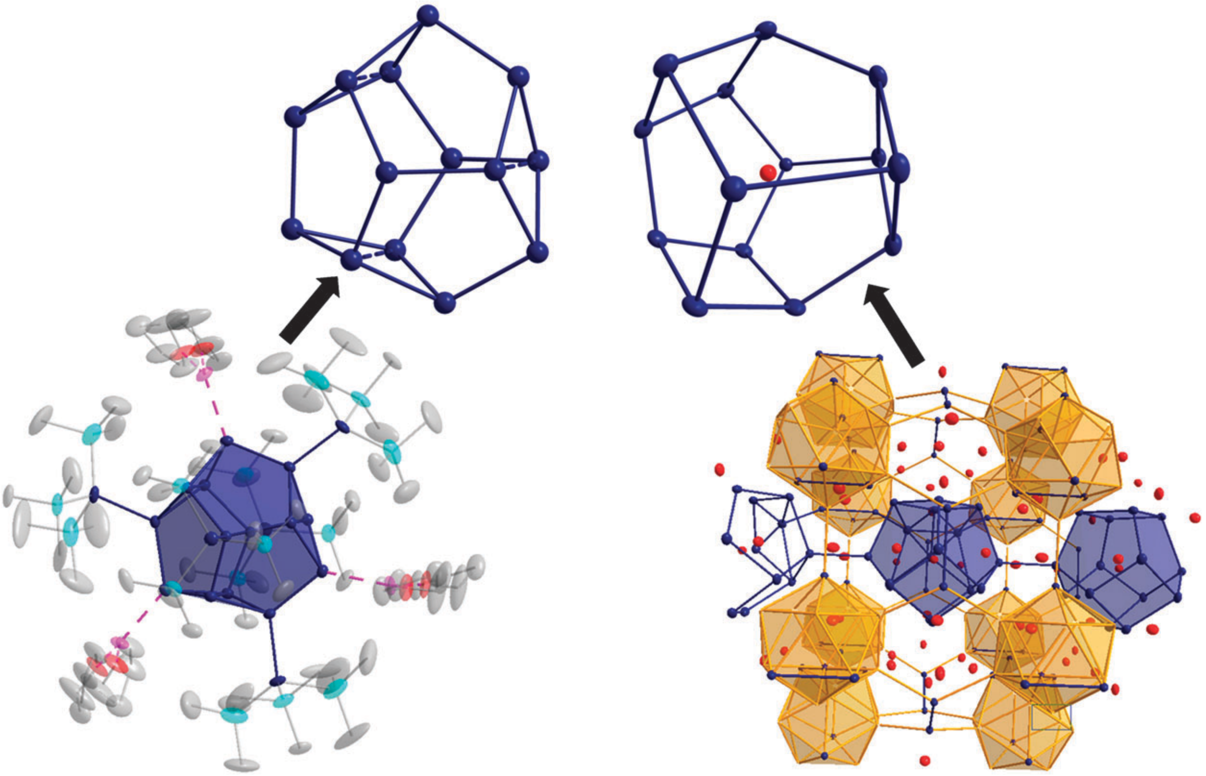

**Fig. 11** Left: arrangement of the 14 germanium atoms in $(THF)_6Li_3Ge_{14}[Ge(SiMe_3)_3]_5$ **9** and molecular structure of **9** without hydrogen atoms. Right: arrangement of the 14 tin atoms in the Zintl phase $Na_{29}Zn_{24}Sn_{32}$ together with a larger section of this Zintl-phase.

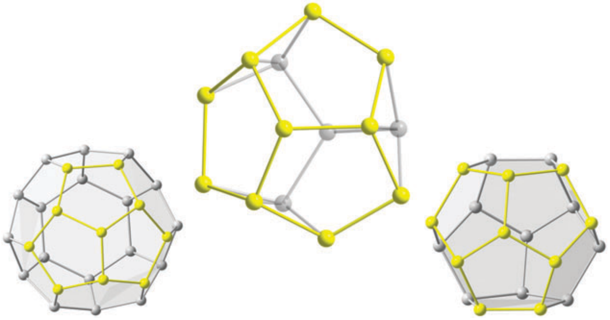

**Fig. 12** Comparison of the substructure of the three directly bound five-membered rings inside the $Ge_{14}$ polyhedron (top) of $(THF)_6Li_3Ge_{14}[Ge(SiMe_3)_3]_5$ **9** with the sub-structure of Ge(*cF*136), hexacaidecahedron (left) and pentagon dodecahedron (right).

## 4. Summary and outlook

Metalloid cluster compounds of germanium of the general formulae $Ge_nR_m$ with $n > m$ represent a new class of germanium cluster compounds. As the average oxidation state of the germanium atoms inside these metalloid clusters is in between 0 and 1, they can be seen as intermediates on the way from oxidized species to the element. Hence the most interesting question is how the bonding situation changes as the average oxidation state approaches the value 0 as in the elemental state. The results available so far, summarized in this review, show that first of all a delocalization of bonding electrons inside the cluster compounds occurs, even in the smallest compound $Ge_5R_4$ **1**. Thus the formation of multiple bonds seems to be unfavourable in metalloid cluster compounds. The results on the $Ge_8R_6$ species **3** and **4** also show a significant dependence between the bonding situation inside the cluster core and the ligand attached.

Further increase in cluster size leads to more delocalized electrons as in a metallic state. This seems quite unusual for the semi-metal germanium and the trend of delocalization might invert in larger clusters leading to elemental germanium with a diamond lattice. Such a transition already occurs at a size of 10 tetrel atoms, as here structures are observed that resemble the atomic arrangement of elemental α-germanium (diamond lattice). Nevertheless, this transition must not necessarily occur as the arrangement of the germanium atoms in the $Ge_{10}$ core inside $(THF)_{18}Na_6Ge_{10}[Fe(CO)_4]_8$ **8** can be interpreted as a structural transition from α- to β-germanium. As β-germanium is a high pressure metallic modification this indicates that also high pressure arrangements with high coordination numbers are possible. The structure of the largest structurally characterized metalloid cluster compound of germanium $(THF)_6Li_3Ge_{14}[Ge(SiMe_3)_3]_5$ **9** shows that also open structures might form on the way to elemental germanium without a stabilizing atom in the centre. Consequently also fullerene-like compounds might be accessible for germanium.

In future experiments it will be necessary to synthesize more and larger metalloid cluster compounds of germanium as well as of the other group 14 elements[63] to shed more light onto this new area of group-14 cluster chemistry. This will lead to a deeper understanding of the development of the bonding situation on the way to the elemental state that is the first step to a structure–property relation in this area and of great significance for nanotechnology. Thus an understanding of the photoluminescence of germanium nanoparticles on a molecular scale might be possible and this is the most exciting and most difficult question to be answered in the future.

## Acknowledgements

I am grateful to the Deutsche Forschungsgemeinschaft for financial support and I would like to thank Prof. Schnöckel and Dipl. Chem. Claudio Schrenk for helpful discussions and calculations.

## Notes and references

1 Group 14 is of particular interest as the module size in computer industry reaches more and more the nanometre range and only recently it was shown that field effect transistors can be built using silicon nanowires; P. Yang, *Dalton Trans.*, 2008, 4387–4391.
2 H. Schnöckel, *Dalton Trans.*, 2005, 3131–3136.
3 D. Barr, W. Clegg, R. E. Mulvey and R. Snaith, *J. Chem. Soc., Chem. Commun.*, 1984, 79–80; N. W. Mitzel and C. Lustg, *Z. Naturforsch., B: Chem. Sci.*, 2001, **56**, 443–445.
4 De-L. Long, R. Tsunashima and L. Cronin, *Angew. Chem.*, 2010, **122**, 1780–1803 (*Angew. Chem., Int. Ed.*, 2010, **49**, 1736–1758).
5 J. F. Corrigan, O. Fuhr and D. Fenske, *Adv. Mater.*, 2009, **21**, 1867–1871.
6 A. Schnepf and H. Schnöckel, Group 13 Chemistry—From Fundamentals to Application, *ACS Symp. Ser.*, 2002, **822**, 154–167.
7 A. Schnepf and H. Schnöckel, *Angew. Chem.*, 2001, **113**, 734–737 (*Angew. Chem., Int. Ed.*, 2001, **40**, 712–715); A. Schnepf, B. Jee, H. Schnöckel, E. Weckert, A. Meents, D. Lübbert, E. Herrling and B. Pilawa, *Inorg. Chem.*, 2003, **42**, 7731–7733.
8 A. Schnepf and H. Schnöckel, *Angew. Chem.*, 2002, **114**, 3682–3704 (*Angew. Chem., Int. Ed.*, 2002, **41**, 3532–3554).
9 J. Hagel, M. T. Kelemen, G. Fischer, B. Pilawa, J. Wosnitza, E. Dormann, H. v. Löhneysen, A. Schnepf, H. Schnöckel, U. Neisel and J. Beck, *J. Low Temp. Phys.*, 2002, **129**, 133–142; O. N. Bakharev, D. Bono, H. B. Brom, A. Schnepf, H. Schnöckel and L. J. de Jongh, *Phys. Rev. Lett.*, 2006, **96**, 117002; D. Bono, A. Schnepf, J. Hartig, H. Schnöckel, G. J. Nieuwenhuys, A. Amato and L. J. de Jongh, *Phys. Rev. Lett.*, 2006, **97**, 077601; D. Bono, O. N. Bakharev, A. Schnepf, J. Hartig, H. Schnöckel and L. J. de Jongh, *Z. Anorg. Allg. Chem.*, 2007, **633**, 2173–2177.
10 However, in other phases (β, γ, or amorphous) Ga is known to show much higher transition temperatures of up to 8.6 K and also a size dependence of $T_c$ for α- and β-phase fine Ga particles was found; W. Buckel and R. Hilsch, *Z. Phys.*, 1954, **138**, 109–120; K. Ohshima and T. Fujita, *J. Phys. Soc. Jpn.*, 1986, **55**, 2798–2802.
11 P. D. Jadzinsky, G. Calero, C. J. Ackerson, D. A. Bushnell and R. D. Kornberg, *Science*, 2007, **318**, 430–433.
12 J. R. Health, J. J. Shiang and A. P. Alivisatos, *J. Chem. Phys.*, 1994, **101**, 1607–1615.
13 A. Lechtken, C. Neiss, M. M. Kappes and D. Schooss, *Phys. Chem. Chem. Phys.*, 2009, **11**, 4344–4350; E. Oger, R. Kelting, P. Weis, A. Lechtken, D. Schooss, N. R. M. Crawford, R. Ahlrichs and M. M. Kappes, *J. Chem. Phys.*, 2009, **130**, 124305-1–124305-10.
14 Another large class of polyhedral cluster compounds of group 14, the Zintl anions and their rich chemistry, are not included in this review, which focuses on metalloid cluster compounds of germanium, where the germanium atoms are positively charged. In the case of the Zintl anions the germanium atoms are negatively charged and therefore they are obtained from the element by adding electrons (reduction), while metalloidclusters are obtained by oxidation.[43] Consequently, metalloid clusters and Zintl anions are separated by the elemental state. The similarities and differences between these two groups of polyhedral group 14 cluster compounds are not discussed as this would go beyond the scope of this review. For recent reviews on the fascinating chemistry of Zintl anions see: J. D. Corbett, *Angew. Chem.*,

2000, **112**, 682–704 (*Angew. Chem., Int. Ed.*, 2000, **39**, 670–690); T. F. Fässler, *Coord. Chem. Rev.*, 2001, **215**, 347–377; S. C. Sevov and J. M. Goicoechea, *Organometallics*, 2006, **25**, 5678–5692.

15 *Holleman–Wiberg Lehrbuch der Anorganischen Chemie*, ed. N. Wiberg, E. Wiberg and A. Holleman, de Gruyter & Co., Berlin, 102nd edn, 2007, pp. 1002–1041.

16 P. Villars, *Pearson's Handbook of Crystallographic Data for Intermetallic Phases*, Desk Edition, ASM International, Materials Park, OH, USA, 1997.

17 R. J. Nelmes, M. I. McMahon, N. G. Wright, D. R. Allan and J. S. Loveday, *Phys. Rev. B: Condens. Matter*, 1993, **48**, 9883–9886.

18 J. S. Kasper and S. M. Richards, *Acta Crystallogr.*, 1964, **17**, 752–755.

19 A. M. Guloy, R. Ramlau, Z. Tang, W. Schnelle, M. Baitinger and Y. Grin, *Nature*, 2006, **443**, 320–323.

20 This result impressively demonstrates the difference between metalloid clusters and Zintl anions: hence in the case of the Zintl anions the oxidation leads to the elemental state while in the case of the metalloid cluster the elemental state is reached *via* reduction, being exactly the opposite reaction.[43]

21 G. S. Armatas and M. G. Kanatzidis, *Nature*, 2006, **441**, 1122–1125.

22 D. Sun, A. E. Riley, A. J. Cadby, E. K. Richmann, S. D. Korlann and S. H. Tolbert, *Nature*, 2006, **441**, 1126–1130.

23 D. C. Paine, C. Caragianis, T. Y. Kim and Y. Shigesato, *Appl. Phys. Lett.*, 1993, **62**, 2842–2844; H. Yang, X. Wang, H. Shi, S. Xie, F. Wang, X. Gu and X. Yao, *Appl. Phys. Lett.*, 2002, **81**, 5144–5146.

24 Y. Maeda, N. Tsukamoto, Y. Yazawa, Y. Kanemitsu and Y. Masumoto, *Appl. Phys. Lett.*, 1991, **59**, 3168–3170; H. Yang, R. Yang, X. Wan and W. Wan, *J. Cryst. Growth*, 2004, **261**, 549–556.

25 A. F. Richards, M. Brynda, M. M. Olmstead and P. P. Power, *Organometallics*, 2004, **23**, 2841–2844.

26 A. F. Richards, H. Hope and P. P. Power, *Angew. Chem.*, 2003, **115**, 4205–4208 (*Angew. Chem., Int. Ed.*, 2003, **42**, 4071–4074).

27 A. Schnepf and R. Köppe, *Angew. Chem.*, 2003, **115**, 940–942 (*Angew. Chem., Int. Ed.*, 2003, **42**, 911–913).

28 A. Schnepf and C. Drost, *Dalton Trans.*, 2005, 3277–3280.

29 A. Schnepf, *Angew. Chem.*, 2003, **115**, 2728–2729 (*Angew. Chem., Int. Ed.*, 2003, **42**, 2624–2625).

30 A. Sekiguchi, Y. Ishida, Y. Kabe and M. Ichinohe, *J. Am. Chem. Soc.*, 2002, **124**, 8776–8777.

31 A. Schnepf, *Chem. Commun.*, 2007, 192–194.

32 A. Schnepf and C. Schenk, *Angew. Chem.*, 2006, **118**, 5499–5502 (*Angew. Chem., Int. Ed.*, 2006, **45**, 5373–5376).

33 C. Schenk and A. Schnepf, *Chem. Commun.*, 2008, 4643–4645.

34 "Naked" here doesnot mean isolated, that is interaction-free, but is merely a linguistic simplification to distinguish the different types of metal atoms in these clusters. Alternatively the metal atoms could also be termed ligand-free. However, this description is equally inexact since bonded metal atoms can also be classified as ligands.

35 N. Wiberg, W. Hochmuth, H. Nöth, A. Appel and M. Schmidt-Amelunxen, *Angew. Chem.*, 1996, **108**, 1437–1438 (*Angew. Chem., Int. Ed. Engl.*, 1996, **35**, 1333–1334).

36 A. Sekigushi, C. Kabuto and H. Sakurai, *Angew. Chem.*, 1989, **101**, 97–98 (*Angew. Chem., Int. Ed. Engl.*, 1989, **28**, 55–56).

37 A. Sekigushi, T. Yatabe, H. Kamatani, C. Kabuto and H. Sakurai, *J. Am. Chem. Soc.*, 1992, **114**, 6260–6262.

38 R. Köppe and A. Schnepf, *Z. Anorg. Allg. Chem.*, 2002, **628**, 2914–2918.

39 P. L. Timms, *Cryochemistry*, Wiley, New York, 1976, pp. 61–136.

40 A. Ecker, E. Weckert and H. Schnöckel, *Nature*, 1997, **387**, 379–381.

41 These subsequent reactions open the way to larger aggregates on the way to novel materials: C. Schenk and A. Schnepf, *Angew. Chem.*, 2007, **119**, 5408–5410 (*Angew. Chem., Int. Ed.*, 2007, **46**, 5314–5316); C. Schenk, F. Henke, G. Santigo, I. Krossing and A. Schnepf, *Dalton Trans.*, 2008, 4436–4441; C. Schenk and A. Schnepf, *Chem. Commun.*, 2009, 3208–3210; F. Henke, C. Schenk and A. Schnepf, *Dalton Trans.*, 2009, 9141–9145.

42 K. Koch, A. Schnepf and H. Schnöckel, *Z. Anorg. Allg. Chem.*, 2006, **632**, 1710–1716.

43 C. Schenk, F. Henke, M. Neumaier, M. Olzmann, H. Schnöckel and A. Schnepf, *Z. Anorg. Allg. Chem.*, DOI: 10.1002/zaac.201000034.

44 This behavior is different to another class of subvalent compounds of group 14, where multiple bonds are formed leading to a novel chemistry, which has lately been reviewed; P. Power, *Nature*, 2010, **463**, 171–177.

45 A. Sekiguchi, T. Fukawa, V. Ya. Lee, M. Nakamoto and M. Ichinohe, *Angew. Chem.*, 2003, **115**, 1175–1177 (*Angew. Chem., Int. Ed.*, 2003, **42**, 1143–1145).

46 C. Schenk, C. Drost and A. Schnepf, *Dalton Trans.*, 2009, **5**, 773–776.

47 F. Breher, *Coord. Chem. Rev.*, 2007, **251**, 1007–1043.

48 Additionally, the bonding situation in **3** and **4** can be described primarily according to Wade's rules,[49] as it is mostly the case for the Zintl anions. Hence, the octahedral shape of **3** can be traced back to a *closo* cluster bonding situation, as $2n + 2$ bonding electrons are present inside the cluster core. For **4** a *nido* structure is to be expected, as $2n + 4$ bonding electrons are present in the cluster core. However, in the case of **4** the *closo* structure of a tricapped trigonal prism seems to be energetically more favorable, leading to a large edge/high value of 1.27 for the trigonal prism as expected for a *closo* cluster of nine atoms with $2n + 4$ skeletal electrons.[50].

49 K. Wade, *Adv. Inorg. Chem. Radiochem.*, 1976, **18**, 1–66.

50 M. E. O'Neill and K. Wade, *Polyhedron*, 1983, **2**, 963–966.

51 M. Brynda, R. Herber, P. B. Hitchcock, M. F. Lappert, I. Nowik, P. P. Power, A. V. Protchenko, A. Ruzicka and J. Steiner, *Angew. Chem.*, 2006, **118**, 4439–4443 (*Angew. Chem., Int. Ed.*, 2006, **45**, 4333–4337).

52 The structural feature of **6** and **7** was additionally observed in the cluster anion $Au_3Ge_{45}{}^{9-}$, that was synthesized from the Zintl-anion $Ge_9{}^{4-}$, showing that this arrangement of germanium atoms is important in the borderlandbetween molecules and the solid state even at the reductive side; [14]A. Spiekermann, S. D. Hoffmann, T. F. Fässler, I. Krossing and U. Preiss, *Angew. Chem.*, 2007, **119**, 5404–5407 (*Angew. Chem., Int. Ed.*, 2007, **46**, 5310–5313).

53 C. Rocaniere, J. P. Laval, P. Dehaudt, B. Gaudreau, A. Chotard and E. Suard, *J. Solid State Chem.*, 2004, **177**, 1758–1767.

54 A. Schnepf and H. Schnöckel, *Angew. Chem.*, 2002, **114**, 3682–3704 (*Angew. Chem., Int. Ed.*, 2002, **41**, 3532–3554).

55 C. Schrenk, I. Schellenberg, R. Pöttgen and A. Schnepf, *Dalton Trans.*, 2010, **39**, 1872–1876.

56 U. Schwarz, *Z. Kristallogr.*, 2002, **219**, 376–390.

57 To calculate the volume of a cluster, first of all the experimentally determined coordinates of the naked metal atom core are taken; *i.e.*, $Ge_{10}$ (from $(THF)_{18}Na_6Ge_{10}[Fe(CO)_4]_8$ **8**). These coordinates are then used as an input for a HF/3-21G* single point calculation (GAUSSIAN03).[57] Using the thereby obtained gas-phase SCF-orbitals the IPCM solvation model (Isodensity Surface Polarized Continuum Model) then constructed an iso(electron)density surface around the metal core (isodensity value = 0.0004 e $Å^{-3}$). In the output file the volume enclosed within this surface is given. This volume, divided by the number of atoms, is the atomic volume used in the discussion. The same calculations are made for a $Ge_{10}$ (adamantine-like) cut-out of the solid state structure of α-germanium. J. B. Foresmann, T. A. Keith, K. B. Wiberg, J. Snoonian and M. J. Frisch, *J. Phys. Chem.*, 1996, **100**, 16098–16104; M. J. Frisch, G. W. Trucks, H. B. Schlegel, G. E. Scuseria, M. A. Robb, J. R. Cheesman, V. G. Zakrzewksi, J. A. Montgomery, R. E. Stratmann, J. C. Burant, S. Dapprich, J. M. Millam, A. D. Daniels, K. M. Kudin, M. C. Strain, O. Farkas, J. Tomasi, V. Barone, M. Cossi, R. Cammi, B. Mennucci, X. Pomelli, C. Adamo, S. Clifford, J. Ochterski, G. A. Petersson, P. Y. Ayala, Q. Cui, K. Korokuma, D. K. Malick, A. D. Rabuck, K. Raghavachari, J. B. Foresman, J. Cioslowski, J. V. Prtiz, B. B. Stefanov, G. Liu, A. Liashenko, P. Pislorz, I. Komaromi, R. Gomperts, R. L. Martin, D. J. Fox, T. Keith, M. A. Al-Laham, C. Y. Peng, A. Nanayakkara, C. Gonzalez, M. Challacombe, P. M. W. Gill, B. G. Johnson, W. Chen, M. W. Wong, J. L. Andres, M. Head-Gordon, W. S. Replogle and J. A. Pople, Gaussian, Inc., Pittsburgh, PA, 2001.

58 A. Donchev, A. Schnepf, G. Stößer, E. Baum, H. Schnöckel, T. Blank and N. Wiberg, *Chem.–Eur. J.*, 2001, **7**, 3348–3353.

59 Li–O distances in $Li(THF)_4^+$ are 192 pm *e.g.* in $\{Ge_9[Si(SiMe_3)_3]_3\}^-\cdot Li(THF)_4$.[29]

60 The arrangement might be described as "inverse tetrahedrally" as introduced by Wiberg *et al.* for the metalloid silicon compound $Si_8(SitBu_3)_6$; G. Fischer, V. Huch, M. S. K. Vasisht, M. Veith and N. Wiberg, *Angew. Chem.*, 2005, **117**, 8096–8099 (*Angew. Chem., Int. Ed.*, 2005, **44**, 7884–7887).

61 L. R. Sita and R. D. Bickerstaff, *J. Am. Chem. Soc.*, 1989, **111**, 6454–6456; C. Drost, M. Hildenbrand and P. Lönnecke, *Main Group Met. Chem.*, 2002, **25**, 93–98; A. F. Richards and P. P. Power, *Organometallics*, 2004, **23**, 4009–4011; D. Nied, W. Klopper and F. Breher, *Angew. Chem.*, 2009, **121**, 1439–1444 (*Angew. Chem., Int. Ed.*, 2009, **48**, 1411–1416).

62 S.-J. Kim, S. D. Hoffman and T. F. Fässler, *Angew. Chem.*, 2007, **119**, 3205–3209 (*Angew. Chem., Int. Ed.*, 2007, **46**, 3144–4148).

63 A. Schnepf, *Chem. Soc. Rev.*, 2007, **36**, 745–758.